

Development of Multilayer Rectangular Coils for Multiple-Receiver Multiple-Frequency Wireless Power Transfer

Chaoqiang Jiang*, Kwok Tong Chau, Wei Han, and Wei Liu

Abstract—In this paper, three viable multilayer rectangular coil structures, namely the spiral, concentrated and uneven compound types, are proposed and analyzed. In the multiple-receiver multiple-frequency wireless power transfer system, the compact coil topologies are particularly preferable and should fulfill the required performance of magnetic field with the compact size design. In order to minimize the variation of magnetic fields that can be picked up by multiple receivers, the uneven compound type is newly derived by combining the merits of both the spiral and concentrated types. Because of providing more uniform magnetic flux density distribution, the uneven compound type can achieve better tolerance of misalignment. Without any misalignment, its transmission efficiency can reach up to 92%. Moreover, their electric potential distributions are analyzed to provide guidance for the maximum input current at the desired operation frequency. Both finite element analysis and experimental results are given to verify the validity of the proposed coil structures.

1. INTRODUCTION

In recent ten years, wireless power transfer (WPT) has been regarded as one of the most prominent technologies and also attracted substantial attention from academic research and industrial business [1–3]. The WPT technique has been successfully adopted in many daily life applications, such as medical implants [4], portable electronics [5], and electric vehicle (EV) charging [6–8]. In addition, some emerging applications are getting popular by utilizing WPT technique to realize the properties of more flexibility and robust [9, 10], such as for wireless motoring [11], wireless heating [12] and wireless lighting [13]. The corresponding definite advantages are high safety, high reliability, low maintenance, and electrical isolation [14–16], which are particularly important for modern EVs [17]. In particular, the wireless power transfer for move-and-charge could effectively alleviate the problem of short driving range per charge of the battery EV [18].

The key element in the WPT system is a pair of magnetically coupled coils — transmitter and receiver coils which are tuned at the same resonant frequencies [19]. When wirelessly delivering power over a long distance, multiple-receiver coils can be adopted in which the resonant coils between the transmitter and receiver coils serve as the repeaters [20, 21]. Also, in the multiple-frequency WPT system, a single transmitter can be used to feed multiple-receiver coils with different resonant frequencies [22, 23]. And then the targeted power transmission can be achieved to improve the system flexibility. Usually, the coreless planar coil is preferable to achieve better ability of tolerance to misalignment than that with ferrite core [24]. Also, using several coreless planar subcoils as one coil for multiple-receiver application can achieve better efficiency and power transmission ability [25]. Since the circular coil has the problem of limited coverage, the rectangular coil is preferable in the multiple-receiver WPT system [26]. However, in order to provide the desired power transfer capability, the size

Received 2 June 2018, Accepted 29 July 2018, Scheduled 2 August 2018

* Corresponding author: Chaoqiang Jiang (cqjiang@eee.hku.hk).

The authors are with the Department of Electrical and Electronic Engineering, The University of Hong Kong, Pokfulam, Hong Kong, China.

of this kind of system is usually very large and thus the system flexibility is reduced. Normally, a single-layer planar coil is used for both the transmitter and receiver, which will significantly increase the system complexity and occupied volume.

In order to adapt the transmitter design to multiple-receiver applications, this paper proposes the design and analysis of multilayer rectangular coil structures. For those multiple-receiver WPT systems, the compact size and good power transfer capability are especially desired. Besides, the uniform magnetic field distribution over the transmitter should be considered to make sure that the mutual inductances of the multiple receivers are the same. Three viable types of multilayer rectangular coils, namely the spiral type, concentrated type, and uneven compound type will be investigated. Apart from assessing their magnetic field distributions using finite element analysis (FEA), the corresponding electric potential distributions will be analyzed at various currents to provide the guidance for selection and arrangement. Also, experimental results will be given to verify the proposed coil structures.

2. SYSTEM CONFIGURATION AND OPERATION

The multiple-receiver multiple-frequency WPT system is shown in Figure 1, which consists of one transmitter with three switched-capacitors to selectively feed three receivers with different resonant frequencies for transmission. This WPT system has been applied to wireless DC motor drives [4], which highly desires a multilayer rectangular coil structure. In order to balance the mutual inductances of the receivers to the transmitter, the transmitter coil is required to produce uniform magnetic field. Three multilayer rectangular coil structures are proposed as shown in Figure 2, which are the spiral type, the concentrated type and the uneven compound type. These three coil types can be applied to both the transmitter and receiver.

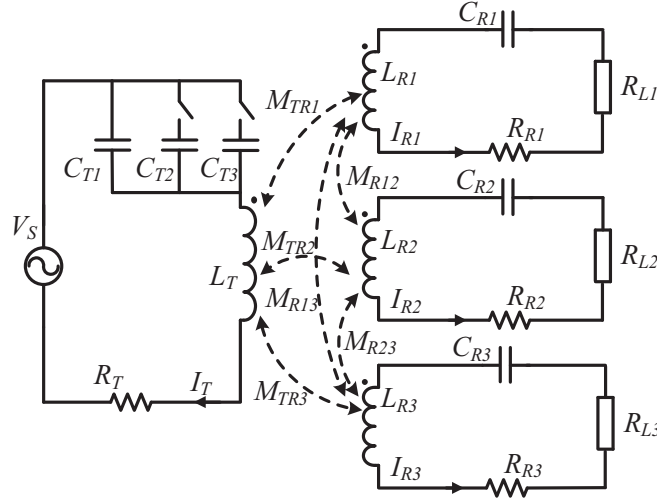


Figure 1. Multiple-receiver multiple-frequency WPT system.

2.1. Multiple-Receiver WPT

As shown in Figure 1, the system involves the AC input voltage V_S , the compensated switched-capacitor array C_{Ti} ($i = 1, 2, \text{ and } 3$), three receivers with the inductance L_i and load resistance R_{Li} , in which R_T , L_T are the resistance and inductance of the transmitter coil, C_{Ri} and R_{Ri} are the capacitance and resistance of each receiver coil, I_T and I_{Ri} are the currents of the transmitter and each receiver, and M_{TRj} is the mutual inductance between the transmitter coil and each receiver coil. The mutual inductances between two receiver coils M_{Rij} ($j = 1, 2, \text{ and } 3$) are ignored because they are arranged on the same plane. When there are obvious gaps between every two receivers' resonant frequencies, the received power can be easily controlled by the transmitter operating frequency. In other word, once the transmitter is tuned to a particular receiver's resonant frequency, only that receiver can pick up most

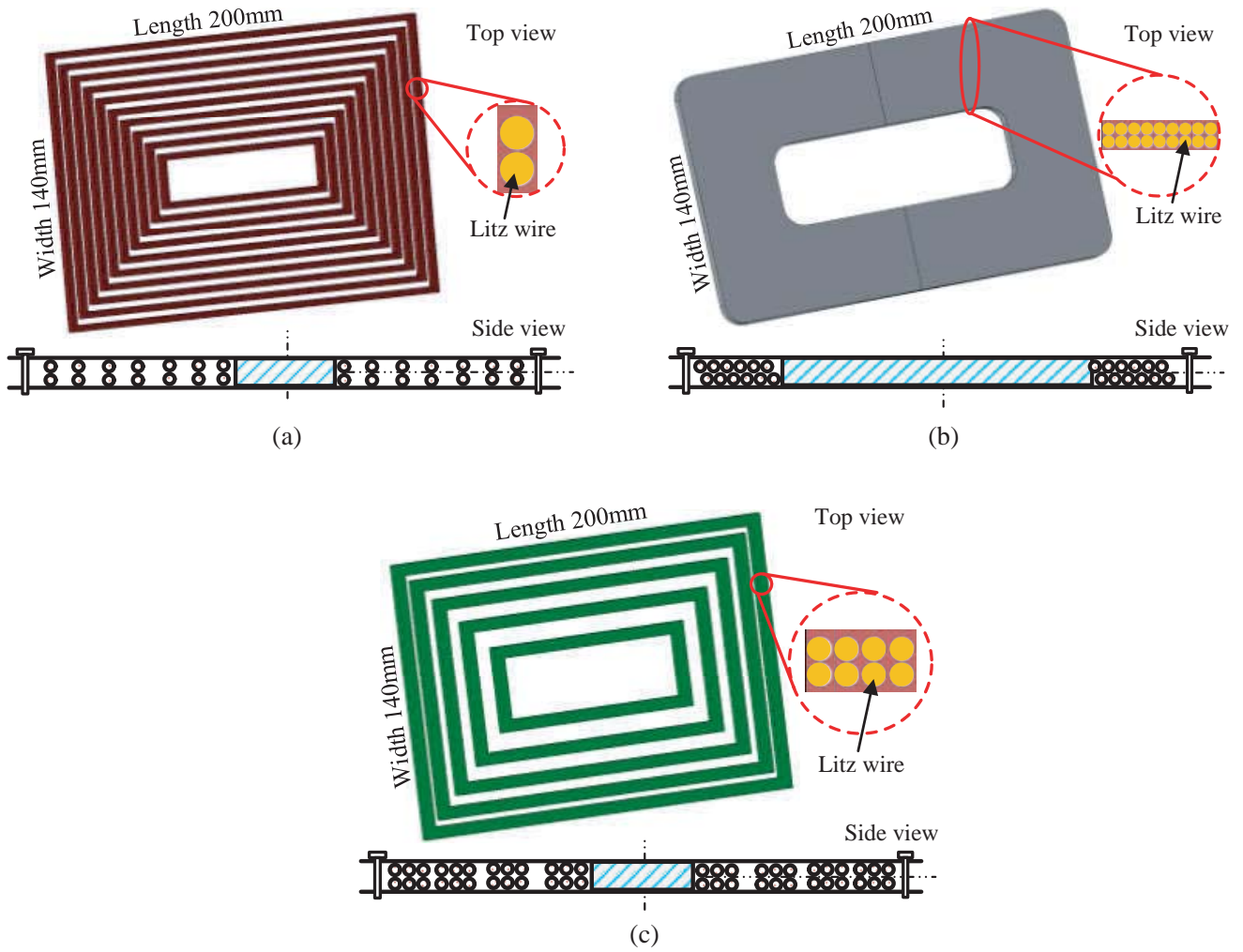


Figure 2. Proposed multilayer rectangular coil structures: (a) Spiral type. (b) Concentrated type. (c) Uneven compound type.

wireless power, whereas other two receivers can only pick up insignificant power. Hence, the system equation can be expressed as:

$$\begin{cases} Z_T I_T + j\omega M_{TR1} I_{R1} + j\omega M_{TR2} I_{R2} + j\omega M_{TR3} I_{R3} = V_S \\ j\omega M_{TR1} I_T + (Z_{R1} + R_{L1}) I_{R1} + j\omega M_{R12} I_{R2} + j\omega M_{R13} I_{R3} = 0 \\ j\omega M_{R12} I_{R1} + j\omega M_{TR2} I_T + (Z_{R2} + R_{L2}) I_{R2} + j\omega M_{R23} I_{R3} = 0 \\ j\omega M_{R13} I_{R1} + j\omega M_{R23} I_{R2} + j\omega M_{TR3} I_T + (Z_{R3} + R_{L3}) I_{R3} = 0 \end{cases} \quad (1)$$

where ω represents the angular frequency, and Z_N is the resultant reactance in the loop N ($N = T, R1, R2,$ and $R3$) which is equal to $j(\omega L_N - 1/(\omega C_N)) + R_N$.

When the operating frequency of the transmitter is tuned to the resonant frequency of receiver i , the transmitted power P_{IN} and the received power P_{OUT_i} for the load resistance R_{Li} can be expressed as

$$\begin{cases} P_{IN} = V_S I_T = \left| \frac{V_S^2 (Z_{Ri} + R_{Li})}{(M_{TRi} \omega)^2 + Z_T (Z_{Ri} + R_{Li})} \right| \\ P_{OUT_i} = I_{Ri}^2 R_{Li} = \left| \frac{M_{TRi}^2 \omega^2 V_S^2 R_{Li}}{((M_{TRi} \omega)^2 + Z_T (Z_{Ri} + R_{Li}))^2} \right| \end{cases} \quad (2)$$

Thus, the system transmission efficiency can be calculated by

$$\eta = \frac{P_{OUTi}}{P_{IN}} = \left| \frac{M_{TRi}^2 \omega^2 R_{Li}}{((M_{TRi} \omega)^2 + Z_T(Z_{Ri} + R_{Li}))(Z_{Ri} + R_{Li})} \right| \quad (3)$$

As a result, the system transmission efficiency and power transfer capability can be written as

$$(\eta, P) = f \left(\begin{matrix} M_{TRi}, L_T, L_{Ri}, \\ \omega, R_T, R_{Ri}, R_{Li} \end{matrix} \right) \quad (4)$$

For exemplification, the key parameters are listed in Table 1. The transmission efficiency can be calculated with respect to different resonant frequencies and mutual inductances. As depicted in Figure 3, it can be observed that the system transmission efficiency increases with the increase of mutual inductance. Thus, by improving the coupling between the transmitter and the receiver, the system transmission efficiency can be significantly improved. Besides, the higher the operating frequency, the higher the transmission efficiency can be observed. Nevertheless, higher operating frequency will cause higher electric potential, which inevitably needs a larger gap between two coil turns.

Table 1. Practical system parameters.

Item	Value	Unit
Resonant frequencies (f_j)	50, 75, 100	kHz
Resistance of transmitter coil (R_T)	0.85	Ω
Resistance of receiver coil (R_{Rj})	0.5	Ω
Load resistance (R_{Li})	20.0	Ω
Inductance of transmitter (L_T)	0.37	mH
Inductance of receiver (L_{Ri})	0.18	mH

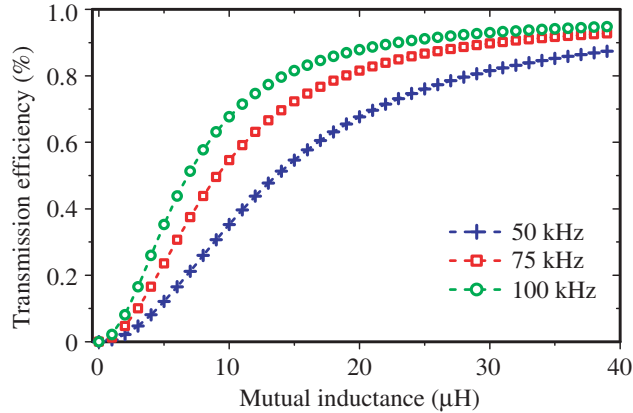


Figure 3. Calculated transmission efficiency at different resonant frequencies.

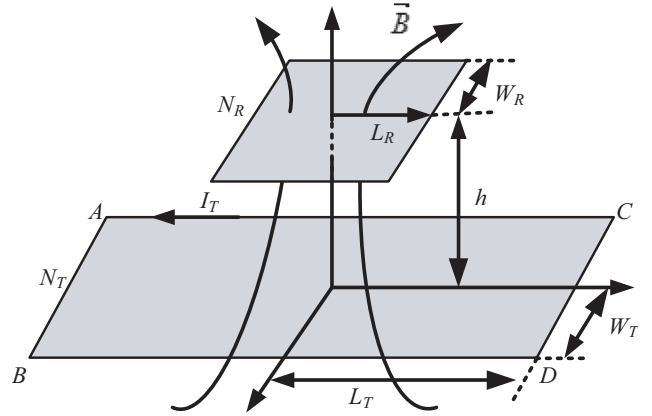


Figure 4. Magnetic flux of single-turn rectangular filament coil.

2.2. Multilayer Rectangular Coils

In order to optimize the system transmission efficiency, the coil inductance and mutual inductance should be further improved. On the other hand, for the multiple-receiver WPT system, the variations of magnetic flux lines through the receivers should be reduced. In the proposed three coil structures, as shown in Figure 2, the peripheral dimensions are 200 mm and 140 mm. The Litz wire with 165×0.1 mm

is adopted to make up all coils. For the spiral type, all turns of the coil are distributed evenly with two layers. Meanwhile, for the concentrated type, all turns of the coil are bundled together with two layers. By combining the advantageous features of both the spiral type and concentrated type, the uneven compound type is proposed where five turns form one bundle with two layers and the pitch distances between every two bundles are not the same, namely, $S_1 = 3$ mm, $S_2 = 5$ mm, and $S_3 = 7$ mm. Once the system parameters are predefined, the mutual inductance between the transmitter and receiver becomes the major determinant of the system performances such as transmission efficiency and power transfer capability.

As shown in Figure 4, the mutual inductance between the transmitter and the receiver is determined by magnetic flux through the receiver coil. For each loop coil, the mutual inductance can be calculated by the total magnetic flux Ψ_{TR} excited by the transmitter current I_T as given by

$$M_{TR} = \frac{\psi_{TR}}{I_T} = \frac{\iint \vec{B} d\vec{S}_R}{I_T} \tag{5}$$

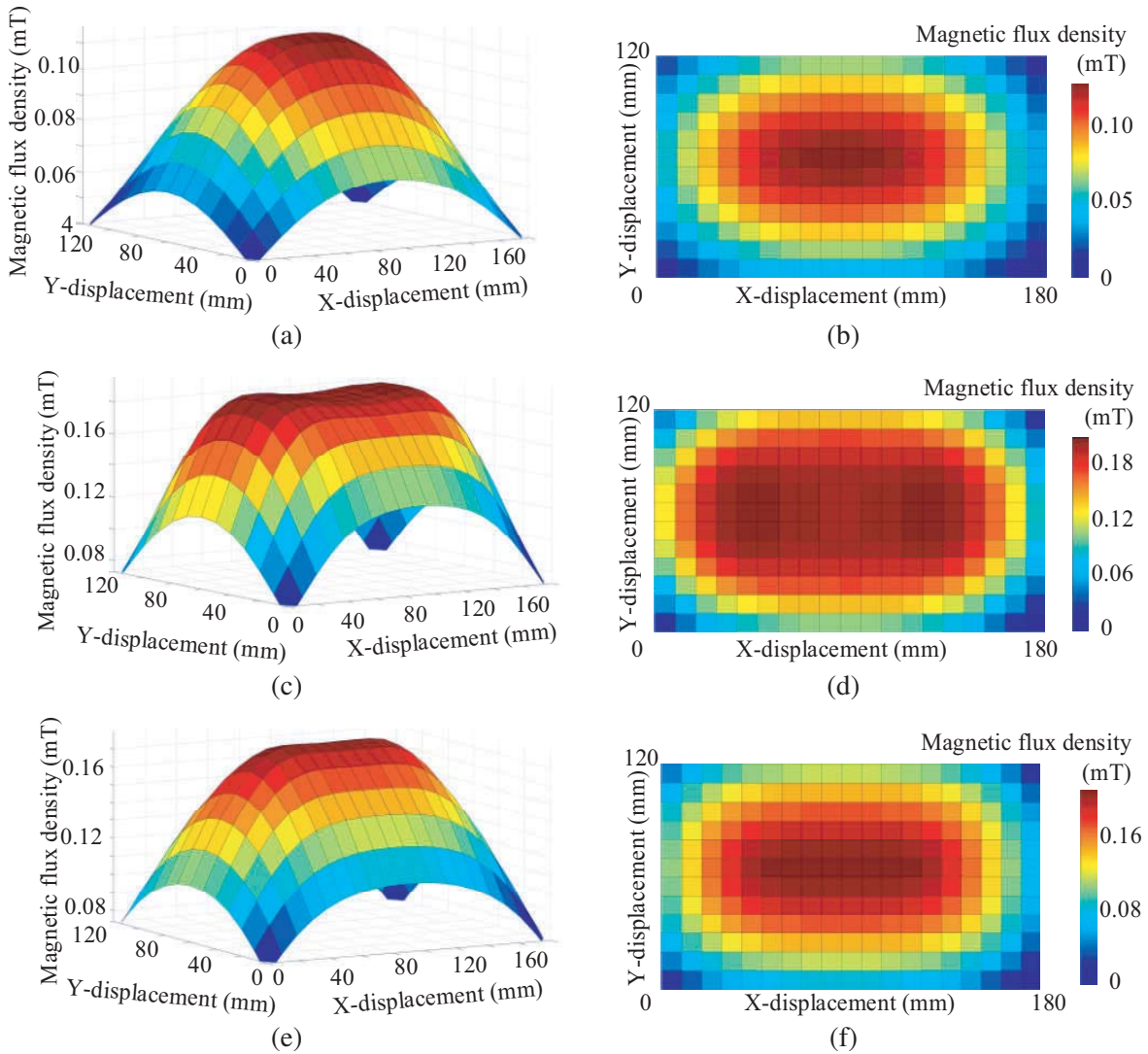


Figure 5. Magnetic field distributions. (a) Spiral type-side view. (b) Spiral type-top view. (c) Concentrated type-side view. (d) Concentrated type-top view. (e) Uneven compound type-side view. (f) Uneven compound type-top view.

where \vec{B} represents the magnetic flux density of magnetic field, and \vec{S}_R is the effective area of receiver coil.

In the proposed three coil structures, each turn can be regarded as a filament and then the total mutual inductance can be obtained by summing the mutual inductances of all turns as given by

$$M_{TR\text{Total}} = \sum_i M_{TR}(LT_i) \quad (6)$$

As a result, when the transmitter can provide the same magnetic flux density for multiple receivers on the same plane, the mutual inductances between the transmitter and receivers can be kept the same. Moreover, the uniform magnetic flux density can help improve the ability of misalignment tolerance.

3. SIMULATION AND ANALYSIS

Based on the same peripheral dimensions of the proposed three coil structures with two layers of 40 turns, the outer width of 140 mm, the outer length of 200 mm, and every 5 turns for each loop of the uneven compound type, the magnetic field distributions and electric potential distributions of all three types of coils are analyzed by using the finite element analysis (FEA) based software JMAG.

3.1. Magnetic Field Analysis

Figure 5 shows the magnetic field distributions of the proposed multilayer rectangular coil structures. The spiral type essentially provides a frustum-like magnetic field distribution as depicted in Figures 5(a) and (b). Both the concentrated and uneven compound types provide the rectangular flat-top magnetic field distributions as depicted in Figures 5(c), (d) and (e), (f), respectively. Although the concentrated type provides the magnetic flux density of 0.18 mT, which is slightly higher than the uneven compound type with 0.17 mT, the magnetic field of the compound type is more uniform than that of the concentrated type. This can be further illustrated by assessing the magnetic field distributions at the middle half plane as shown in Figure 6.

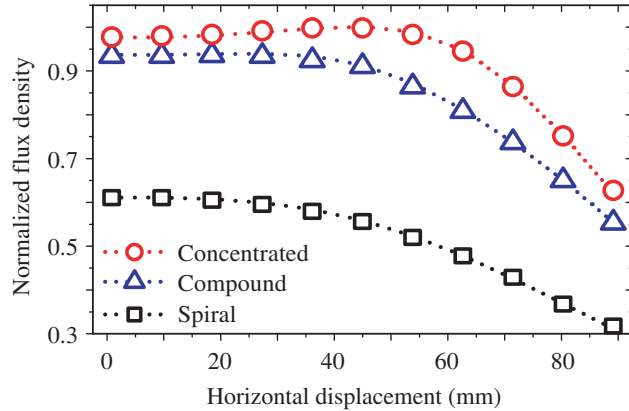


Figure 6. Normalized magnetic flux densities of various transmitter coil structures at middle plane.

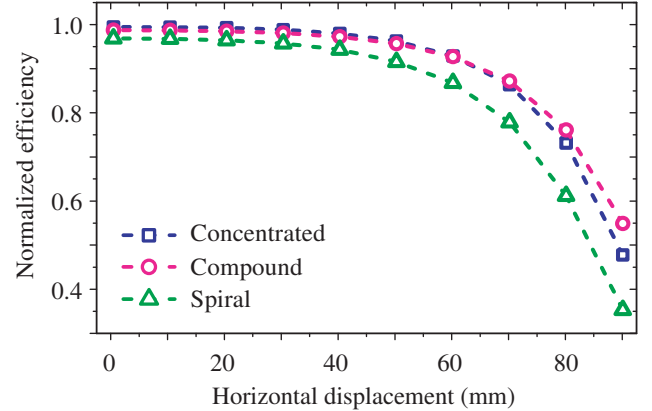


Figure 7. Normalized transmission efficiencies with respect to horizontal displacement.

Moreover, the system transmission efficiencies are calculated when these three coil structures are adopted as the transmitter. As shown in Figure 7, it can be observed that the normalized efficiency of the compound type is only slightly lower than that of the concentrated type within short horizontal displacement while offering more uniform efficiency than that of the spiral and concentrated types along the horizontal displacement.

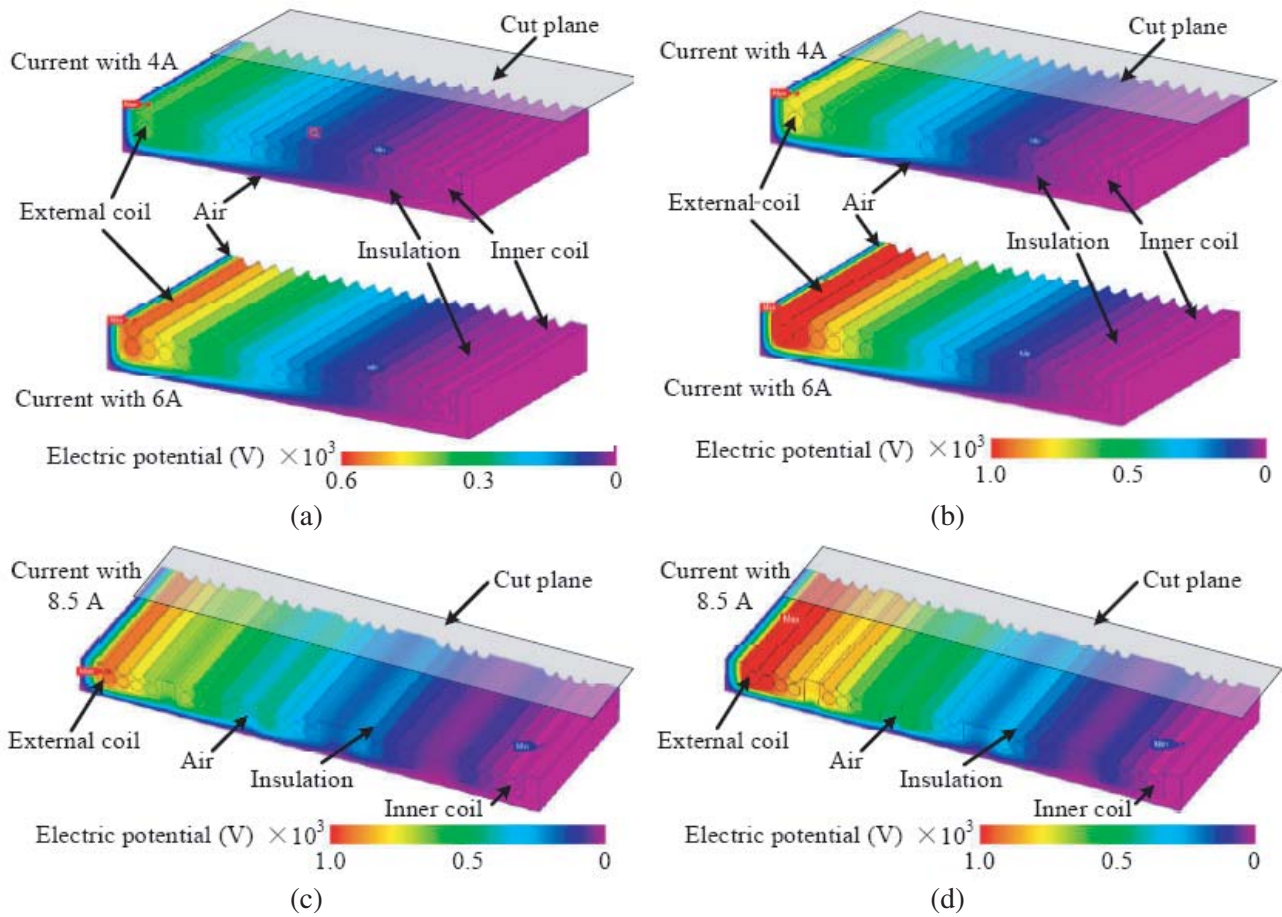


Figure 8. Electric potential distributions. (a) Concentrated type with 50 kHz. (b) Concentrated type with 100 kHz. (c) Uneven compound type with 6 A and 100 kHz. (d) Uneven compound type with 8.5 A and 100 kHz.

3.2. Electric Potential Distributions

For the multilayer coil structure at high-frequency operation, the proximity effect should be analyzed to avoid possible breakdown between two adjacent windings. As shown in Figure 8, the maximum electric potentials of the concentrated type with input currents of 4 A and 6 A at 50 kHz are 380 V and 570 V, respectively, which are far lower than the breakdown potential of 1200 V of the selected Litz wires. When the operation frequency increases to 100 kHz, the maximum electric potentials with 4 A and 6 A are increased to 760 V and 1150 V, respectively. It indicates that the input current of 6 A is the threshold value for the 100 kHz operation in order to avoid the Litz wires from possible breakdown. The electric potential distributions of the uneven compound type are shown in Figures 8(c) and (d). It can be observed that the maximum electric potential of the compound type coil with the input current of 6 A is lower than that of the concentrated type. For the same breakdown voltage, a higher current threshold value of 8.5 A can be achieved due to the lower self-inductance of the uneven compound type. It should be noted that these contour plots are created by utilizing the static electric field analysis built in the FEA based JMAG. As illustrated in Figure 8, a cut plane is located at the upper half coil so as to directly display the electric potentials of the coil, insulation and air region. Also, it should be noted that the input current of the WPT system generally decreases with the increase of the operation frequency. Similar findings occur at the spiral and uneven compound types.

4. EXPERIMENTAL VALIDATION

An experimental setup is built as shown in Figure 9 in which the programmable function generator is used to drive the wideband power amplifier to produce the desired AC power, the oscilloscope (Lecroy 6100 A) is used to measure currents and then calculate the efficiency, the magnetic flux density is measured by seven magnetic sensors (TMR 2001), and all data are recorded by the data acquisition board (NI USB-6225) and displayed by LabVIEW NXG. The operation frequency is set at 95 kHz according to practical parameters.

For experimentation, the testing power is set at 12 W, and all magnetic sensors are distributed at the height of 35 mm. As shown in Figure 10(a), both the measured magnetic flux density and load power of the uneven compound type vary slightly within the horizontal displacement of 40 mm. For the simulated and measured magnetic flux density distributions in the central area within the horizontal displacement of 40 mm, they are almost the same. When the horizontal displacement becomes larger, there is a discrepancy between the simulation and experimental results due to the larger flux leakage of the handmade coil winding.

Moreover, the corresponding mutual inductance and transmission efficiency are measured as shown in Figure 10(b). Generally, the efficiencies in both the simulation and experiment will be reduced with the increase of displacement. It should be noted that the coil-to-coil efficiencies in the simulation and experimental results are different. This is because of the nature of different supply sources, namely the

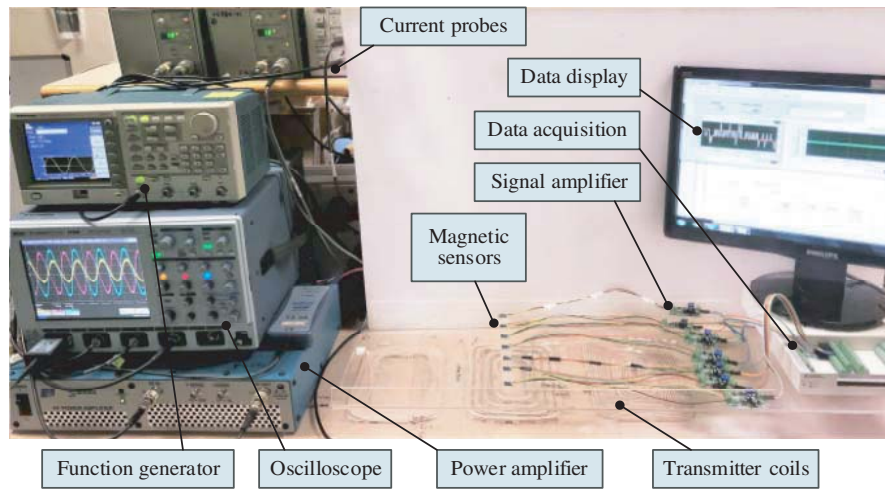


Figure 9. Experimental setup.

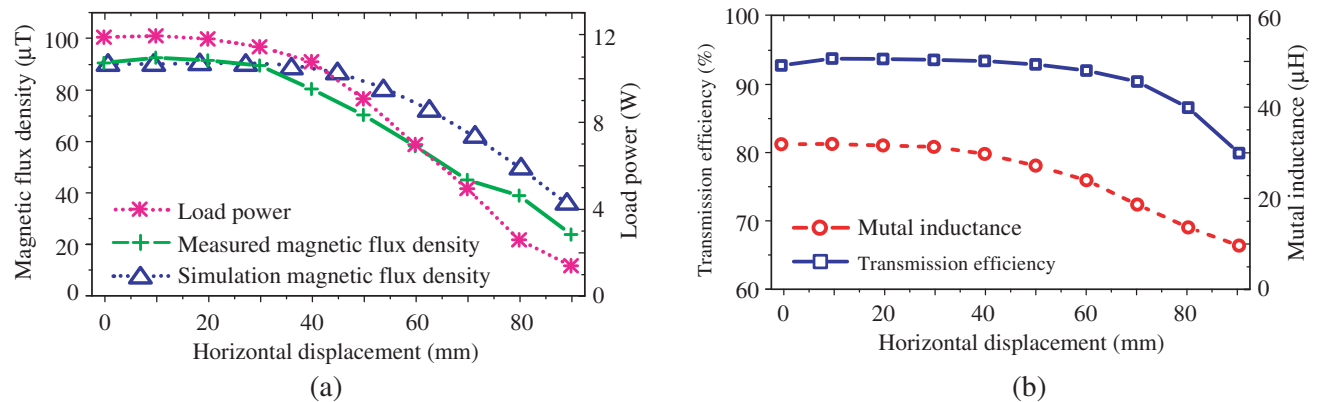


Figure 10. Simulation and experimental results of uneven compound type. (a) Magnetic flux density and load power. (b) Transmission efficiency and mutual inductance.

idealized constant current source is used in the simulation whereas the practical constant voltage source is adopted in the experiment. Without any misalignment, the transmission efficiency can reach up to 92% with the transmission distance of 35 mm. When the transmitter and receiver are not centrally aligned, the mutual inductance starts to vary with the displacement. It can be found that the mutual inductance can almost keep at the same value within 40 mm displacement. Therefore, the compound coil type can provide more uniform magnetic field and hence better tolerance of misalignment.

5. CONCLUSION

In this paper, three multilayer rectangular coil structures have been proposed for the multiple-receiver multiple-frequency WPT system. Among them, the uneven compound type can provide more uniform magnetic flux density distribution, hence minimizing the difference of magnetic fields that can be picked up by multiple receivers. Moreover, its electric potential distribution is analyzed to determine the maximum input current at the desired operation frequency. Both finite element analysis and experimental results can well verify the validity of the proposed coil structures. In particular, the measured transmission efficiency of the proposed uneven compound type can achieve up to 92%.

ACKNOWLEDGMENT

This work was supported by a grant (Project No. 17204317) from the Hong Kong Research Grants Council, Hong Kong Special Administrative Region, China.

REFERENCES

1. Covic, G. A. and J. T. Boys, "Inductive power transfer," *Proceedings of the IEEE*, Vol. 101, No. 6, 1276–1289, Jun. 2013.
2. Robichaud, A., M. Boudreault, and D. Deslandes, "Theoretical analysis of resonant wireless power transmission links composed of electrically small loops," *Progress In Electromagnetics Research*, Vol. 143, 485–501, 2013.
3. Jang, B.-J., S. Lee, and H. Yoon, "HF-band wireless power transfer system: Concept, issues, and design," *Progress In Electromagnetics Research*, Vol. 124, 211–231, 2012.
4. Park, S. I., "Enhancement of wireless power transmission into biological tissues using a high surface impedance ground plane," *Progress In Electromagnetics Research*, Vol. 135, 123–136, 2013.
5. Jiang, C., K. T. Chau, C. Liu, and C. H. T. Lee, "An overview of resonant circuits for wireless power transfer," *Energies*, Vol. 10, No. 7, 894:1–20, Jun. 2017.
6. Zhang, Z., H. Pang, A. Georgiadis, and C. Cecati, "Wireless power transfer — An overview," *IEEE Transactions on Industrial Electronics*, 2018, doi: 10.1109/TIE.2018.2835378.
7. Mi, C. C., G. Buja, S. Y. Choi, and C. T. Rim, "Modern advances in wireless power transfer systems for roadway powered electric vehicles," *IEEE Transactions on Industrial Electronics*, Vol. 63, No. 10, 6533–6545, Oct. 2016.
8. Zhang, Z. and K. T. Chau, "Homogeneous wireless power transfer for move-and-charge," *IEEE Transactions on Power Electronics*, Vol. 30, No. 11, 6213–6220, Nov. 2015.
9. Poon, A. S. Y., "A general solution to wireless power transfer between two circular loop," *Progress In Electromagnetics Research*, Vol. 148, 171–182, 2014.
10. Kim, J., W.-S. Choi, and J. Jeong, "Loop switching technique for wireless power transfer using magnetic resonance coupling," *Progress In Electromagnetics Research*, Vol. 138, 197–209, 2013.
11. Jiang, C., K. T. Chau, C. Liu, and W. Han, "Design and analysis of wireless switched reluctance motor drives," *IEEE Transactions on Industrial Electronics*, 2018, doi: 10.1109/TIE.2018.2829684.
12. Han, W., K. T. Chau, Z. Zhang, and C. Jiang, "Single-source multiple-coil homogeneous induction heating," *IEEE Transactions on Magnetics*, Vol. 53, No. 11, 7207706:1–6, Nov. 2017.

13. Jiang, C., K. T. Chau, Y. Y. Leung, C. Liu, C. H. T. Lee, and W. Han, "Design and analysis of wireless ballastless fluorescent lighting," *IEEE Transactions on Industrial Electronics*, 2017, doi: 10.1109/TIE.2017.2784345.
14. Li, C. J. and H. Ling, "Investigation of wireless power transfer using planarized, capacitor-loaded coupled loops," *Progress In Electromagnetics Research*, Vol. 148, 223–231, 2014.
15. Fan, Y., L. Li, S. Yu, C. Zhu, and C.-H. Liang, "Experimental study of efficient wireless power transfer system integrating with highly sub-wavelength metamaterials," *Progress In Electromagnetics Research*, Vol. 141, 769–784, 2013.
16. El Badawe, M. and O. M. Ramah, "Efficient metasurface rectenna for electromagnetic wireless power transfer and energy harvesting," *Progress In Electromagnetics Research*, Vol. 161, 35–40, 2018.
17. Zhang, Z., K. T. Chau, C. Liu, C. Qiu, and T. W. Ching, "A positioning-tolerant wireless charging system for roadway-powered electric vehicles," *Journal of Applied Physics*, Vol. 117, 17B520:1–4, 2015.
18. Chau, K.-T., C. Jiang, W. Han, and C. H. T. Lee, "State-of-the-art electromagnetics research in electric and hybrid vehicles," *Progress In Electromagnetics Research*, Vol. 159, 139–157, 2017.
19. Zhang, Z., K. T. Chau, C. Qiu, and C. Liu, "Energy encryption for wireless power transfer," *IEEE Transactions on Power Electronics*, Vol. 30, No. 9, 5237–5246, Sep. 2015.
20. Ahn, D. and S. Hong, "A study on magnetic field repeater in wireless power transfer," *IEEE Transactions on Industrial Electronics*, Vol. 60, No. 1, 360–371, Jan. 2013.
21. Huang, S., Z. Li, Y. Li, X. Yuan, and S. Cheng, "A comparative study between novel and conventional four-resonator coil structures in wireless power transfer," *IEEE Transactions on Magnetics*, Vol. 50, No. 11, 1–4, Nov. 2014.
22. Jiang, C., K. T. Chau, C. Liu, and W. Han, "Wireless DC motor drives with selectability and controllability," *Energies*, Vol. 10, No. 1, 49:1–15, Jan. 2017.
23. Jiang, C., K. T. Chau, T. W. Ching, C. Liu, and W. Han, "Time-division multiplexing wireless power transfer for separately excited DC motor drives," *IEEE Transactions on Magnetics*, Vol. 53, No. 11, 1–5, Nov. 2017.
24. Qiu, C., K. T. Chau, C. Liu, T. W. Ching, and Z. Zhang, "Modular inductive power transmission system for high misalignment electric vehicle application," *Journal of Applied Physics*, Vol. 117, No. 17, 17B528:1–4, Apr. 2015.
25. Casanova, J. J., Z. N. Low, and J. Lin, "A loosely coupled planar wireless power system for multiple receivers," *IEEE Transactions on Industrial Electronics*, Vol. 56, No. 8, 3060–3068, Aug. 2009.
26. Qiu, C., K. T. Chau, C. Liu, W. Li, and F. Lin, "Quantitative comparison of dynamic flux distribution of magnetic couplers for roadway electric vehicle wireless charging system," *Journal of Applied Physics*, Vol. 115, No. 17, 17A334:1–3, May 2014.